

# TAVP: Task-Adaptive Visual Prompt for Cross-domain Few-shot Segmentation

Jiaqi Yang, Ye Huang, Xiangjian He, Linlin Shen, Guoping Qiu

**Abstract**—Under the backdrop of large-scale pre-training, large visual models (LVM) have demonstrated significant potential in image understanding. The recent emergence of the Segment Anything Model (SAM) has brought a qualitative shift in the field of image segmentation, supporting flexible interactive cues and strong learning capabilities. However, its performance often falls short in cross-domain and few-shot applications. Transferring prior knowledge from foundation models to new applications while preserving learning capabilities is worth exploring. This work proposes a task-adaptive prompt framework based on SAM, a new paradigm for Cross-domain few-shot segmentation (CD-FSS). First, a Multi-level Feature Fusion (MFF) was used for integrated feature extraction. Besides, an additional Class Domain Task-Adaptive Auto-Prompt (CDTAP) module was combined with the segmentation branch for class-domain agnostic feature extraction and high-quality learnable prompt production. This significant advancement uses a unique generative approach to prompts alongside a comprehensive model structure and specialized prototype computation. While ensuring that the prior knowledge of SAM is not discarded, the new branch disentangles category and domain information through prototypes, guiding it in adapting the CD-FSS. We have achieved the best results on three benchmarks compared to the recent state-of-the-art (SOTA) methods. Comprehensive experiments showed that after task-specific and weighted guidance, the abundant feature information of SAM can be better learned for CD-FSS.

**Index Terms**—Cross-domain, Few-shot, Semantic Segmentation, Segment Anything

## I. INTRODUCTION

Traditional deep networks have relied heavily on extensive annotated data to achieve high precision performance [1]. However, data annotation is a time-consuming task that requires significant human resources, especially for the segmentation of intensive pixel-level annotation tasks like medical images and remote sensing images. Therefore, Few-shot semantic segmentation (FSS) was introduced to narrow this gap [2], aiming to reduce the need for labeling. Besides, most of the few-shot learning (FL) methods mainly focus on learning the relationship between support and query sets within the same domain, which always requires fine-tuning on the target domain. The features extracted on the high level are class-agnostic but lack domain generalization, meaning that FL methods have the ability for new category generation but perform worse on new domain generation. The previous methods have limitations in that input-space-based enhancement requires expert knowledge to design enhancement functions, while feature-based enhancement usually relies on complex adversarial training [3]. Thus, Cross-domain Few-shot

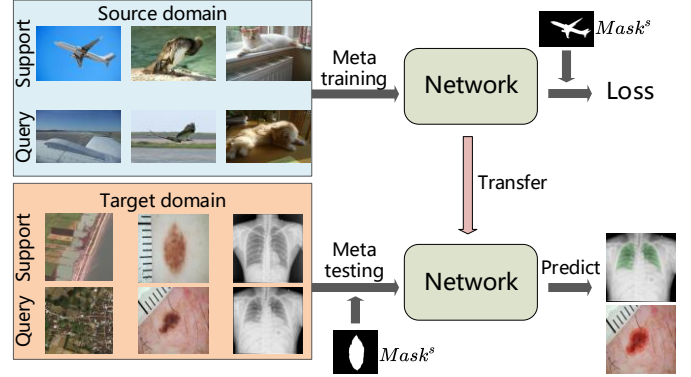


Fig. 1: The existing pipeline of cross-domain few-shot segmentation task.

Segmentation (CD-FSS) [4] came up for solving segmentation tasks on medical, remote sensing, and other images, and four typical cross-domain data sets are illustrated in Figure 1.

However, previous deep models may lead to poor generalization on unseen out-of-domain data, which limits their use in Cross-domain Few-shot scenarios. Recently, Large fundamental visual models (LVM) have made significant progress in natural image segmentation [5]–[7], including medical [8] and remote sensing [9] image segmentation. The Segment Anything Model (SAM) [10] was trained with over one billion masks and achieved unprecedented generalization capabilities on natural images. Additionally, some research has shown that proper adjustments to SAM can be applied in medical image segmentation [8] and zero-shot tasks. These advances suggest that powerful segmentation models with generalization capabilities can be used without designing complex networks as fine-tuning models due to the time-consuming retraining. Some early works have used pre-trained models on natural or medical images and achieved good performance [10], [11]. However, due to the inflexible capacity of pre-trained models and extensive few-shot methods such as disentanglement domain classifier [12], the cross-domain generalization ability of deep models has not been effectively improved.

Although these LVM-based methods have improved the model's performance in some professional domains, SAM does not have the ability to generalize in other vertical domains and requires a large number of vertical domain samples, which brings high expenses in data collection, sample labeling, and model training. At the same time, the vertical domain itself is difficult to exhaustively enumerate. Many works have integrated the SAM framework with meta-learning for transfer

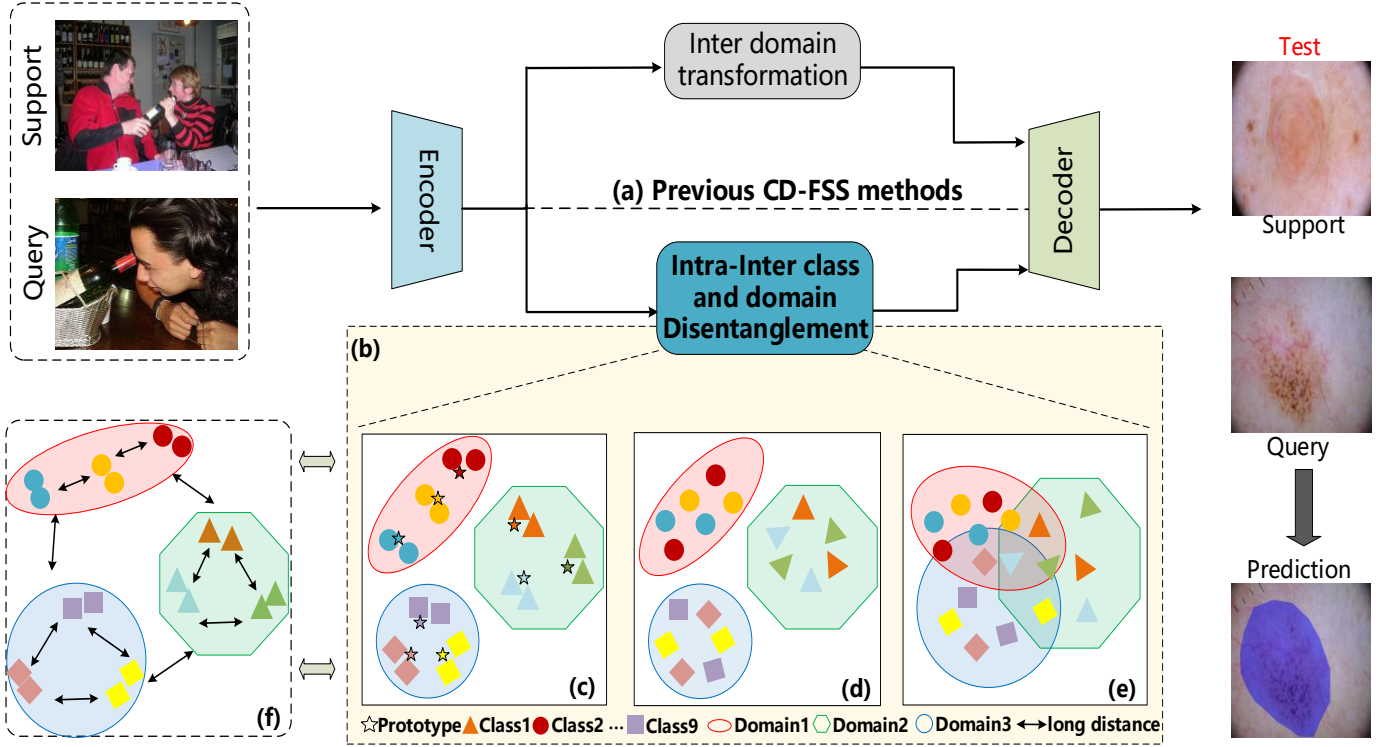


Fig. 2: (a)The existing cross-domain segmentation method based on SAM. (b) Our CDTAP module. (c)Produce class-specific and domain-specific feature. (d)Produce class-agnostic feature. (e)Produce domain-agnostic feature. (f)Original feature distribution.

learning tasks [13], [14]. However, previous methods mainly focus on fine-tuning the SAM encoder, designing teacher-student by knowledge distillation [15], and feature matching by computing the distance between pairs. To increase computing efficiency and to better disentangle features of class and domains for model robust learning ability, we propose a Task-adaptive Visual Prompt (TAVP) algorithm achieving both inter and intra-domain information disentanglement combined with SAM. In contrast, our method can be effectively generalized to different vertical domains and can achieve results comparable to vertical domains. The pipeline comparison is shown in Figure 2.

Upon further analysis of SAM, we identify its poor performance in CD-FSS, which can be attributed to a few key issues. The encoder’s image features, though containing basic class data, are mismatched with the target domain’s categories, with their inherent distributions potentially causing noise and performance drops. Effective learning requires feature information aligned with the target domain. Moreover, the decoder’s reliance on prompt-based cross-attention mechanisms also hinders its segmentation effectiveness.

Based on the above analysis, the CDTAP module is proposed to better extract class and domain-specific features through contrastive learning from foreground and background for improving the robustness of CD-FSS, as shown in Figure 3. The experimental results show that our work can compute more accurate and robust pairing relationships between samples. Moreover, we propose a fully automatic segmentation framework based on SAM for CD-FSS. This

new framework aims to enhance the model’s adaptability and accuracy for CD-FSS. Our contributions can be summarized as follows.

- Compared with SAM, which extracts features in multi-level context, we remain low-level feature representation and capture both global and local information by fusion.
- To realize the disentanglement of class and domain information, we integrate a unified and comprehensive feature transform method. Specifically, an additional Class-Domain Task-adaptive Auto-prompt (CDTAP) module is proposed for domain and class-agnostic feature extraction. Simultaneously, We use contrastive learning to achieve deeper and closer matching of samples among different domains.
- To overcome the shortage of SAM that highly relies on human interaction, we propose an automatic and learnable prompt branch for segmentation tasks as weighted guiding and robust prompt generation.
- We fine-tune SAM with less time and GPU consumption, and a heterogenization sampling strategy is adopted for Task-adaptive guiding segmentation.
- Our method achieves competitive and best results on three benchmarks compared to the state-of-the-art methods on four publicly available CD-FSS data sets.

The overall structure of the paper includes five sections. We briefly list some related technologies in cross-domain and few-shot learning in Section I. The review of related work about cross-domain and few-shot learning is described

in Section II. We describe our method in more detail and show the model performance in Section III. Then, we conduct comprehensive experiments comparing previous methods and the SAM baseline in Section IV and V. Finally, we conclude this paper and discuss the future application prospects in large model-based fine-tune methods in Section VI.

## II. RELATED WORKS

We start this section by introducing a cross-domain segmentation task with its relative technology, and the few-shot segmentation task is described for related background. Then, we develop the CDFSS task and the related research within this field.

### A. Domain Adaptation in Segmentation

In recent years, domain adaptation semantic segmentation has made notable progress. Domain adversarial training is utilized to learn domain-invariant representations in features [16]. Hoffman et al. [17] integrated global and local alignment methods with adversarial training. There were also other methods such as distillation loss [18], output space alignment [19], class-balanced self-training [20], and conservative loss [21], proposed according to a predefined curriculum learning strategy [22]. These methods collectively contributed to advancing adaptive semantic segmentation by leveraging information from various domains, ensuring the model's robust performance across diverse and less annotated environments. Suppose the training data originate solely from a single domain and adaptation occurs to an unseen domain. Then, in this case, single-source domain adaptation becomes more challenging due to the limited diversity within the training domain. Consequently, a prevalent approach to address this issue is using data augmentation techniques to generate new domains, thereby enhancing the diversity and information content of the training data. Several methods were designed with varying generation strategies to address the single-source domain adaptation problem in computer vision tasks. For example, RandConv [23] employed random convolutions for data augmentation. MixStyle integrated style information from instances of randomly selected different domains.

In contrast with the above data augmentation methods, we use the foundation model to ensure rich prior knowledge instead of generating many images in the source domain, saving computing resources and increasing computation efficiency.

### B. Few Shot Segmentation

The objective of Few-Shot Segmentation (FSS) tasks is to segment new semantic objects through a limited number of available labeled images or unlabeled images that are semantically distinct. Current methods primarily focused on improvements during the meta-learning phase. Prototype-based methods [24]–[26] utilized a technique where representative foreground or background prototypes were extracted from the support data, and various strategies were employed to interact between different prototypes or between prototypes and query features. Relation-based methods [27]–[29] also

succeeded in few-shot segmentation. HSNet [30] built a high correlation using multi-scale dense matching and captures contextual information using 4D convolution. RePRI [31] introduced transductive inference of base class feature extraction that did not require meta-learning. However, these methods primarily focused on segmenting new categories from the same domain. Due to the significant differences in cross-domain distributions, they failed to be extended to unseen domains.

In contrast to the previous computing prototypes from the class level, we propose a Foreground and Background dual prototype matching method, ensuring fine-grained and class-domain agnostic feature representation.

### C. Cross-domain Few-shot Segmentation

There are four benchmarks [4] available for CDFSS standard evaluation. Figure 1 shows the difference between the original domain and CDFSS data sets. It is obvious that for the ChestX data set, the image format has been changed from RGB to gray, with a large gap from the original domain. The other two data sets have more edge information requiring high-quality semantic segmentation. RD [32] introduced a novel domain enhancement strategy leveraging a memory mechanism. This approach involved continuously storing domain-style information from the source domain during the training phase. Subsequently, during testing, this stored source information was utilized to enhance the segmentation performance. During testing, source domain information stored in memory was loaded for the target domain feature enhancement. RD [32] offered a direct approach to reduce domain differences and was validated on typical partitioned datasets. For semantic segmentation tasks in autonomous driving applications, PixDA [33] introduced an innovative pixel-by-pixel domain adversarial loss based on three key criteria: (i) aligning the source and target domains for each pixel, (ii) preventing negative transfer on correctly represented pixels, and (iii) regularizing the training of infrequent classes to mitigate overfitting. CDTF [34] achieved cross-domain few-shot segmentation by aligning support and query prototypes. This alignment was realized using an uncertainty-aware contrastive loss and supplemented with a supervised cross-entropy loss and an unsupervised boundary loss as regularization terms. CDTF [34] enabled the model to generalize from the base model to the target domain without requiring additional labels. CDFSS [35] presented a cross-domain few-shot segmentation framework that leveraged learning from natural domains to assist in rare-disease skin lesion segmentation. This approach was particularly valuable when dealing with limited data for common diseases in the target domain.

Putting aside the previous simple computing prototype methods, we combine high-level prototype representation with a foundation model, SAM. Besides, we propose a dual prototype matching method for the foreground and background, ensuring fine-grained feature representation.

## III. PROPOSED METHOD

While SAM can be generalized to more scenarios, even zero-shot situations, it still has some limitations. Firstly,

the original SAM relies on interactive prompts for accurate segmentation in different situations, which can be time-consuming. The second problem is how to transfer more abundant knowledge and key information from LVM methods while maintaining good generalization ability. To address the above two problems, we propose an automatic framework for segmentation with automatic prompts instead of interactive prompts by users. Meanwhile, an additional branch is designed for class and domain-agnostic feature extraction and Task-adaptive prompts generation.

The overall framework for TAVP is shown in Figure 3. The inputs of support and query from the source domain are fed into the SAM encoder for basic feature extraction. Note that we propose a multi-level feature fusion for extensive representation. Meanwhile, one target domain data is fed into the CDTAP module for class and domain specific and agnostic feature extraction. At the same time, this module generates learnable prompts as dense embedding input to the decoder. Then, the combined multi-level and dense prompts are fed into the SAM decoder for prediction.

#### A. Problem Definition

In the field of cross-domain few-shot semantic segmentation (CD-FSS), we distinguish between a source domain  $(X_s, Y_s)$ . A target domain  $(X_t, Y_t)$ , with differing input distributions and non-overlapping label spaces, meaning  $X_s \neq X_t$  and  $Y_s \cap Y_t = \emptyset$ . Here, ' $X$ ' signifies the input distribution and ' $Y$ ' denotes the label space. Our methodology involves training and evaluating our model episodically within a meta-learning framework as outlined in [4]. Training episodes consist of a support set and a query set. The support set  $S = (I_i^s, M_i^s)$  from  $i = 1$  to  $K$  includes  $K$  pairs of images and their respective binary masks, with  $I$  representing the  $i$ -th support image and  $M_i^s$  the matching binary mask. The query set, defined as  $Q = (I_i^q, M_i^q)$  from  $i = 1$  to  $K$ , operates similarly. The model is fed with the support set  $S$  and a query set  $I_q$  from a specific class  $c$ , upon which it is tasked with predicting the binary mask  $M_q$  of the query. For testing, the model's effectiveness is gauged by providing it with a new support set and corresponding queries from the target domain.

#### B. Multi-level Features Fusion

**High-level Global Feature Representation.** We propose an advanced approach to enhance the mask resolution in SAM by incorporating efficient token learning. Rather than utilizing the coarse masks generated by SAM directly, our method involves a High-level token alongside a novel mask prediction layer to produce higher-quality masks. In this method, we maintain the original mask decoder of SAM but augment it with a newly defined learnable High-level token with the size of  $1 \times 256$ . This token is combined with the existing output tokens from SAM ( $4 \times 256$ ) and prompt tokens with the size of  $N_{prompt} \times 256$ , serving as the augmented input for the SAM mask decoder. Like the original output token function, the High-level token engages in self-attention with the other tokens and partakes in token-to-image and image-to-token attention processes within each attention layer for

feature refinement. The High-level token utilizes a shared point-wise MLP across decoder layers. After two decoder layers, it comprehensively understands global image semantics and conceals mask information from other output tokens. A novel three-layer MLP is then employed to derive dynamic convolutional kernels from the enriched High-level Token, executing a spatial point-wise operation with the amalgamated High-level feature to generate superior-quality masks.

Our approach trains only the High-level Token and its associated three-layer MLPs to correct inaccuracies in the mask produced by SAM without directly fine-tuning SAM or using a post-refinement network. This method stands in contrast to traditional approaches in high-quality segmentation models. Our extensive testing highlights two primary benefits of this efficient token learning technique: 1) It substantially elevates the mask quality of SAM with only a minimal increase in parameters, thus optimizing the training process in terms of time and data efficiency; and 2) Adaptive token and MLP components prevent overfitting, preserving SAM's zero-shot segmentation performance on new images without knowledge loss.

**Global and Local Feature Fusion.** Accurate segmentation requires input features with global semantic context and precise local boundaries. To enhance mask quality further, we augment the mask decoder features of SAM with both advanced object context and refined edge information. Rather than directly utilizing the mask decoder feature of SAM, we construct new multi-level features by extracting and integrating features from various stages of the SAM model. We first extract detailed low-level edge information from the initial layer's local feature of SAM's ViT encoder with a spatial dimension of  $64 \times 64$ . This feature is obtained from the first global attention block within the ViT encoder, specifically the 6th block of 24 blocks in case of a SAM based on ViT-Large. Then, the last layer's high-level global feature from SAM's ViT encoder, sized at  $64 \times 64$ , provides a comprehensive global image context. Finally, the mask feature within SAM's mask decoder, sized at  $256 \times 256$ , is shared by the output tokens and possesses strong mask shape information. As depicted in Figure 3, we initially upsample the early and final layer encoder features to a spatial size of  $256 \times 256$  via transposed convolution to generate the input high-level features. Following this, we combine these three types of features through element-wise summation after straightforward convolutional processing. This approach of fusing global and local features is straightforward yet effective, producing segmentation results that preserve detail with minimal memory and computational costs. In the experimental section, we further conduct a detailed ablation study to assess the impact of each feature source.

#### C. Task-adaptive Transferring (TAT) Class Domain Task-Adaptive Auto-Prompt (CDTAP)

We improve the model's generalization by performing class-domain prototype information disentanglement and using prior-guided automatic prompts for complete task-adaptive automatic prompts generation. The learnable prompt embedding increases the robustness of SAM and our model.

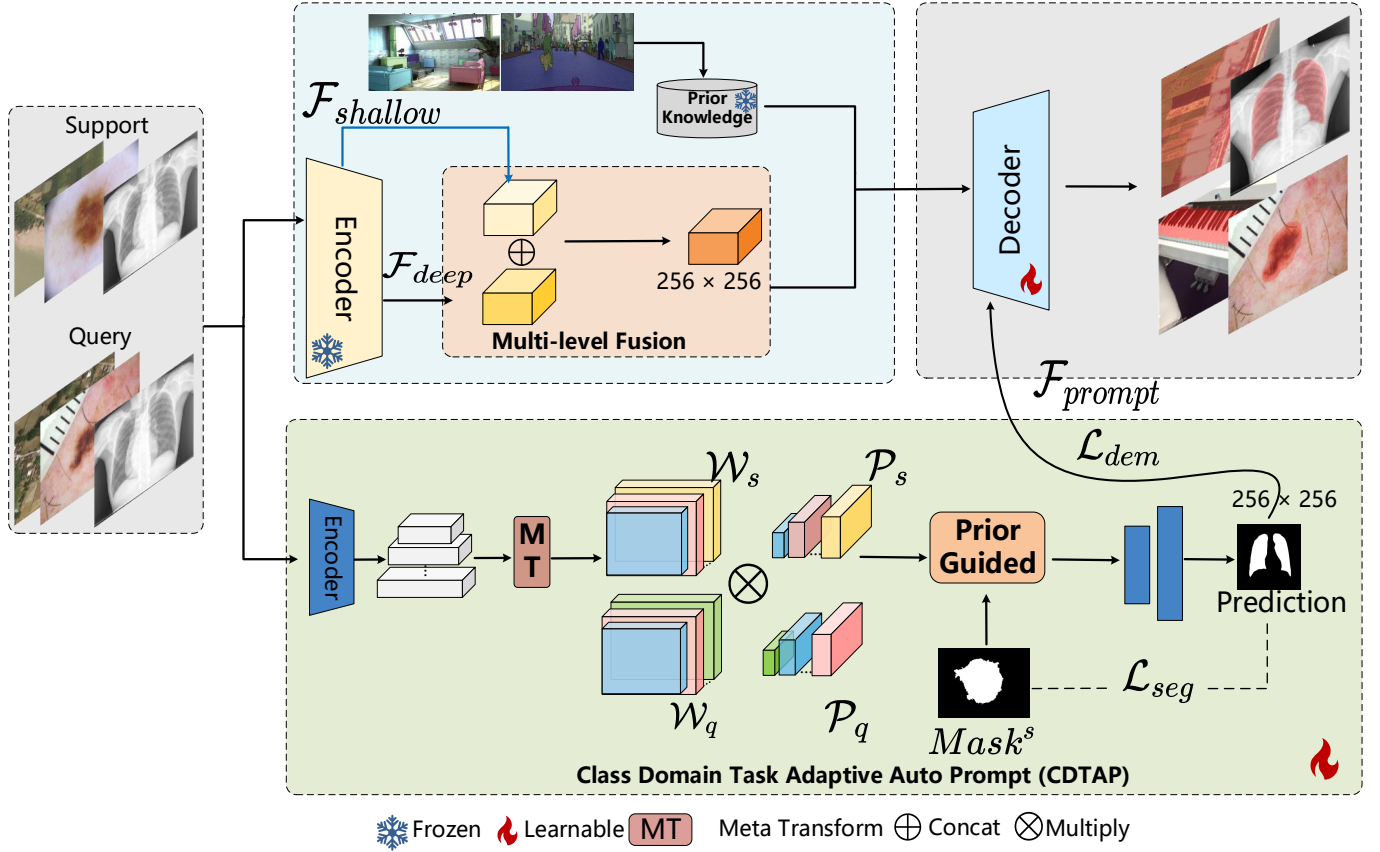


Fig. 3: The overall architecture of proposed TAVP network. First, multi-level features of support and query images are obtained from SAM encoder, then combined with original pre-trained weights on SA-1B dataset [10]. CDTAP is employed for fine-tuning and meta transform. Simultaneously, dense embedding:  $F_{prompt}$  and image embeddings were acquired as the input that fed into decoder. At last, the mask decoder predicts the query image. The  $L_{dem}$  loss is used for learnable prompts supervision and fine-tuning, and the  $L_{seg}$  is used for supervising auto-prompts generation.

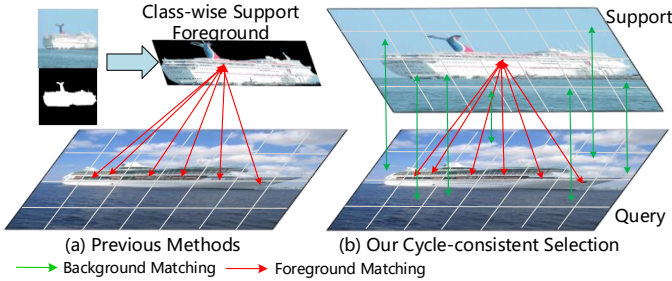


Fig. 4: (a) The previous class-wise few-shot methods. (b) Our two-way matching meta-learning module.

#### Class Domain Prototype Information Disentanglement.

Previous meta-learning methods only have generalizations for new categories, but the performance is poor when faced with both cross-domain and few-shot tasks. Therefore, we propose a new prototype-based class-domain information disentanglement module. To better explore the correlation between different class and domain features for distinct components, class-domain-common and class-domain-specific, we add a branch for the foreground and background prototype calculations. Using pixel-level prototype calculations can make fuller use of

feature representation, which is helpful in few-shot learning. Previous methods only rely on the support prototype set and anchor layer to calculate the transformation matrix. Due to intra-class variance, the support prototype cannot represent all the information in the category. Therefore, we propose to enhance the set of supported prototypes by querying the prototypes. We specifically focus on dual prototype enhancement and cross-domain feature transformation. We leverage cycle consistency between support and query functions to obtain query foreground and background prototypes. Based on these enhanced prototypes that can represent categories and their surroundings, learnable domain-agnostic modules can be used to compute efficient transformation matrices. The transformation matrix is then applied to the query features for cross-domain feature transformation. Representational archetypes are important for our cross-domain transformation. To this end, we construct a pixel-level fine-grained self-cycling supervision that reasons the query foreground and background to support enhancement. We perform forward matching to obtain the query features with the highest similarity to the supporting prospects. We then use these identified forward-matching query features to backward retarget the corresponding supporting features. If the supporting features found by



reverse matching fall within the true supporting foreground mask, the identified query features are averaged and used to derive the foreground prototype. An enhanced background prototype is obtained through the same process. Assuming that  $W$  represents the weight matrix of original features in the Anchor layer and  $P$  represents the prototype of the foreground representation. Specifically, we use equation 1 to get  $P$  from  $W$  and  $A$ . The difference between our algorithm and HQ-SAM [36] for Multi-level features lies in the design of CDTAP module, which transfers the original multi-scale based on feature computation to multi-scale based on prototype computation.

$$WP = A \quad [4] \quad (1)$$

Where  $W$  is a learnable weight matrix,  $P$  is the computed prototypes and  $A$  is a representation matrix calculated from the distance between the center and other features. The prototype of foreground and background can be calculated by Equation 2

$$P_{f,b} = \left[ \frac{P_f}{\|P_f\|}, \frac{P_b}{\|P_b\|} \right] \quad (2)$$

$$i^{s \rightarrow q} = \operatorname{argmax}(\operatorname{sim}(P_f^s \odot P_m^s), P_f^q) \quad (3)$$

$$j^{q \rightarrow s} = \operatorname{argmax}(\operatorname{sim}(P_{i^{s \rightarrow q}}^{q,f}, P_{j^{q \rightarrow s}}^{s,f}), \quad (4)$$

where  $i$  and  $j$  are rows and columns of 2D spatial positions of the feature map, Equation 3 and Equation 4 are the cycling check process.  $P_f^s$  is the prototype representation of an image and  $P_m^s$  is the prototype representation of its mask,  $\odot$  represents the multiplication between vectors.  $P_{i^{s \rightarrow q}}^{q,f}$  is the feature prototype of the query from support to query matching. The corresponding interpretation can be deduced for  $P_{j^{q \rightarrow s}}^{s,f}$ . Given the based equations, the prototype representation of the query can be selected.

We perform class-domain information disentanglement by completing class-domain agnostic feature transformation. Thus, in this branch, we can compute the transformation matrix  $A$  for input by calculating its foreground prototype given its corresponding mask in the Anchor layer. In  $l_{th}$  layer,  $m$  represents the mask,  $C$  represents the class,  $H$  represents its height, and  $W$  is the width. The foreground prototype of the support set can be calculated by

$$p_{s,f}^l = \frac{\sum_i \sum_j f_{s,f}^{l,i,j} \phi^l(m_{s,f}^{i,j})}{\sum_i \sum_j \phi^l(m_{s,f}^{i,j})}, \quad (5)$$

where  $p_{s,f}^l \in R^{C_l}$ ,  $i$  and  $j$  are rows and columns of 2D spatial positions of the feature map,  $\phi(\cdot)$  denotes a function that bilinearly interpolates input tensor to the spatial size of the feature map  $f_{s,f}^{l,i,j}$  at intermediate layer  $l$  by expanding along channel dimension, and  $\phi(\cdot) : R^{H \times W} \rightarrow R^{C_l \times H_l \times W_l}$ ,  $m_{s,f}^{i,j}$  is the foreground prototype from support of mask. The support and query sets' background prototypes can be calculated similarly.

**Prior Guided Learnable Prompts.** An essential advantage of SAM is the support of prompt input. However, it is time-consuming for humans to generate interactive prompts, and the decoder of SAM is always coupled with image and prompt embedding. It is reasonable that the prediction can be more

accurate with higher-quality prompts. This work proposes the generation of prior-guided meta-space learnable prompts. First, the features are mapped to a new space through the previous two-way enhanced prototype information disentanglement, and the most similar features and their label representations calculated in the query set from the support set are used as prior guides to generate prompts. Then, the enhanced inputs, including multi-level image embeddings with the size of  $256 \times 256$  and high-quality prompts of similar size, are fed into a high-quality decoder. After the experiments, we prefer

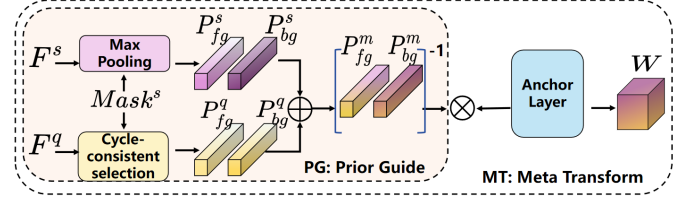


Fig. 5: Details of MT and PG.

that not only the CDFSS task rely on better guidance and representation of foreground and essential information for the input sample, but also the background plays a critical role in more accurate predictions. For example, the more random the background setting is, or the greater the difference between the data in the source domain, the better the model performs.

#### D. Light-Weight Fine-tune Framework

Besides, we adopt a random heterogenization sampling strategy to distinguish different cross-domain tasks. In this strategy, a threshold value is created to supervise the sampling quality. One of the limitations of SAM is that it is time-consuming and inefficient, which is a common issue in large model fine-tuning. In this work, we propose a lighted-weight fine-tuning framework, transferring SAM to cross-domain few-shot segmentation only by re-training a few layers in CNN-based models. First, the target domain samples are fed into the class domain task-specific branch for class-agnostic feature extraction. These highly structured class-agnostic feature embeddings, combined with other feature embeddings from the base domain, are fed into the decoder. A weighted supervision loss is proposed to fine-tune the decoder to predict masks for target domain samples.  $L_{seg}$  represents the segmentation loss function, composed of the Cross-Entropy loss function [37], and a Dice loss function [38], as defined in

$$L_{seg} = (1 - \lambda) \cdot L_{CE} + \lambda \cdot L_{Dice}, \quad (6)$$

where  $\lambda$  is an adjustable parameter for supervision. Simultaneously, samples from the target domain are fed into a CNN-based model to generate dense embeddings as auto prompts. The dense embedding is obtained from the layer of CNN-based backbones as a weight matrix aligned with a feature map. Then, the dense embedding is multiplied with a combined multi-level feature map and is fed into a decoder, achieving guided decoding for target domain samples. Given an input  $x$ , it is fed into a CNN-based encoder. After down-sampling, a simple decoder follows for up-sampling to generate dense

embedding, aligning with the feature map. The  $L_{dem}$  loss function is adopted to supervise dense embedding, as shown in

$$L_{dem}(x) = L_{BCE}(Z_x, M_x) + L_{Dice}(Z_x, M_x), \quad (7)$$

where  $Z_x$  represents the dense embedding of input  $x$ , and  $M_x$  is the mask of input  $x$ .

Overall, the end-to-end training framework is supervised by the following loss function

$$L = L_{seg} + L_{dem}, \quad (8)$$

where  $L_{seg}$  represents segmentation branch supervision and  $L_{dem}$  is the loss function for dense embedding generating.

#### IV. EXPERIMENTS

In this section, we describe the experimental settings, including ‘Data sets’, ‘Data Pre-processing Strategy’, ‘Models Baseline’, and ‘Implementation Details’.

##### A. Experimental Settings

We first introduce the benchmarks in the CD-FSS. Next, the model baseline, implementation details, and performance visualization are listed.

1) *Data Sets*: In cross-domain few-shot segmentation, four benchmarks are contributed [4].

**Deepglobe.** The Deepglobe data set, described in [39], is a collection of satellite images. It includes pixel-level annotations for seven categories: urban areas, agriculture, rangeland, forest, water, barren land, and an ‘unknown’ category. In total, 803 images in the data set have a consistent spatial resolution of  $2448 \times 2448$  pixels.

We divide each image into six sections to increase the number of testing images and reduce their sizes. As the object categories in this data set have irregular shapes, cutting the images minimally impacts their segmentation. We further filter out images with only one class and those belonging to the ‘unknown’ category. This results in 5,666 images used to report the results, each with a resolution of  $408 \times 408$  pixels.

**ISIC.** The data set identified as ‘document number 1’, as described in references [40], [41], focuses on skin lesion imagery from cancer screenings, containing 2,596 images with a single lesion each. Ground-truth labels are provided solely for the training set. For consistent analysis, images are resized to a standard  $512 \times 512$  pixels from the original  $1022 \times 767$  pixels.

**ChestX.** As discussed in [42], [43], the Chest X-ray data set is tailored for Tuberculosis detection. It comprises a total of 566 X-ray images, each having an original resolution of  $4020 \times 4892$  pixels. These images are sourced from a data set of 58 cases with a Tuberculosis manifestation and 80 cases with normal conditions. Given the large size of the original images, a common practice is to reduce them to a more manageable  $1024 \times 1024$  pixels for further analysis and processing.

**FS1000.** FSS-1000 [44] is a natural image dataset for few-shot segmentation, consisting of 1,000 object classes, each with 10 samples. We used the official split for semantic segmentation in our experiment and reported the results on the official testing set, which contains 240 classes and 2,400 testing images.

2) *Data Augmentation and Sampling Strategy*: In this work, a heterogenization sampling strategy is adopted to reduce the coupling effect of training with a limited data set. In this strategy, a threshold is set to supervise the sampling quality. Specifically, we used a 5-fold validation strategy in the split data set once during the training process. The threshold is computed through the training process to select the samples for model training dynamically.

Besides, several data augmentation methods also used in original SAM baseline are utilized, including adjusting the attributes of images such as brightness, contrast, saturation, etc., randomly flipping along vertical and horizontal levels, and randomly affine transformation.

3) *Models*: The overall framework is based on High-quality Segment Anything [36]. Simultaneously, a task-adaptive auto-prompts branch, together with SAM, is proposed to complete the CDFSS.

4) *Training Setting*: For the training data set, only one image from the target domain including ChestX [2, 15], ISIC [9], FSS-1000 [22], and deepglobe [10] at a time are used respectively with augmentation. For training parameters, the baseline is frozen, which shown as the snowflake logo on Figure3. only the CDTAP module is training.

5) *Implementation Details*: We have designed three backbones for the additional branch except the SAM framework. SAM encoder was adapted for high-level global semantic contexts and low-level local information computing. The full ViT is used for computing in global semantic contexts, and the local low-level features are extracted from the early layer. Besides, a CNN-based encoder, modified for computing prototypes, is used for class-domain agnostic feature extraction, and a small up-sampling method is adopted for dense embedding generation as auto-prompts.

During the training stage, the number of epochs is between 60 and 150. Since there is a large weight pre-trained SAM model, the epochs are smaller for end-to-end training to avoid overfitting. Our experiments can achieve ideal results if the running time is between 2 and 6 hours on NVIDIA A6000 GPU, depending on the number of epochs and validation data sets.

#### V. VISUALIZATIONS

##### A. Comparison with SOTA Methods

Extensive experiments are conducted to compare our method with the state-of-the-art methods. The results showed that we achieved better results on the Deepglobe data set than the latest SOTA performance. Besides, in the other three cross-domain data sets, we achieve better and more competitive and accurate results than the previous methods shown in Table I. Moreover, it is obvious that with a more robust model and flexible learning ability, the prediction is closer to the samples’ original semantics, especially pixel-level information, instead of relying on fixed ground truth, as shown in Figure 6.

##### B. Ablation Study

Given the proposed method, we test the performance of models with different combination strategies. Overall, we

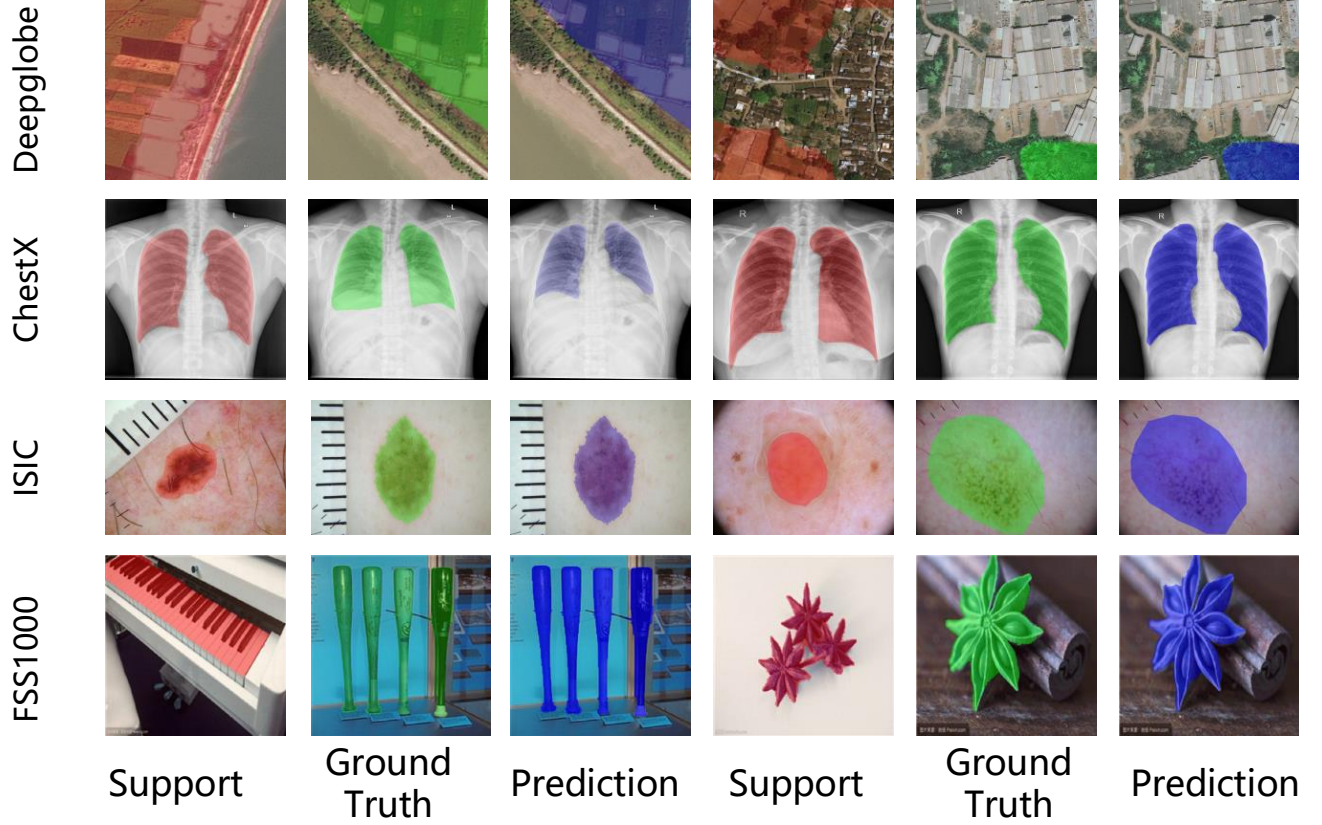


Fig. 6: Qualitative results of TAVP in 1-way 5-shot segmentation on CD-FSS. Support labels are overlaid in red. The ground truth and predictions of query images are in green and blue, respectively.

TABLE I: Comparison with previous FSS and CD-FSS methods under 1-way 1-shot and 5-shot settings on the CD-FSS benchmark.

Methods	Backbone	ISIC		Chest X-ray		Deepeglobe		FSS1000		Average	
Task		1-shot	5-shot	1-shot	5-shot	1-shot	5-shot	1-shot	5-shot	1-shot	5-shot
Few Shot Segmentation Methods											
AMP [45]	VGG-16	28.42	30.41	51.23	53.04	37.61	40.61	57.18	59.24	43.61	45.83
PGNet [29]	ResNet-50	21.86	21.25	33.95	27.96	10.73	12.36	62.42	62.74	32.24	31.08
PANet [2]	ResNet-50	25.29	33.99	57.75	69.31	36.55	45.43	69.15	71.68	47.19	55.10
CaNet [46]	ResNet-50	25.16	28.22	28.35	28.62	22.32	23.07	70.67	72.03	36.63	37.99
RPMMs [28]	ResNet-50	18.02	20.04	30.11	30.82	12.99	13.47	65.12	67.06	31.56	32.85
PFENet [27]	ResNet-50	23.50	23.83	27.22	27.57	16.88	18.01	70.87	70.52	34.62	34.98
RePRI [47]	ResNet-50	23.27	26.23	65.08	65.48	25.03	27.41	70.96	74.23	46.09	48.34
HSNet [48]	ResNet-50	31.20	35.10	51.88	54.36	29.65	35.08	77.53	80.99	47.57	51.38
ViT Based and Cross Domain Few Shot Segmentation Methods											
PATNet [25]	ResNet-50	41.16	53.58	66.61	70.20	37.89	42.97	78.59	81.23	56.06	61.99
RestNet [49]	ResNet-50	42.25	51.10	71.43	73.69	35.68	39.87	81.53	84.89	56.84	62.39
APSeg [50]	ViT	45.43	53.89	84.10	84.50	35.94	39.98	79.71	81.90	61.30	65.09
HQ-SAM [36]	ViT	40.38	47.60	28.76	30.14	24.73	26.82	78.97	80.97	43.21	46.18
SAM-Med2d	ViT	62.37	65.40	65.91	70.85	16.78	18.58	73.54	76.80	54.65	57.91
SAM-Adapter	ViT	33.47	38.33	53.99	58.05	45.79	47.65	67.98	70.80	50.31	53.71
TAVP(ours)	ViT + ResNet	<b>54.89</b>	<b>73.39</b>	70.31	<b>88.61</b>	<b>46.10</b>	<b>61.98</b>	79.09	<b>83.41</b>	<b>62.60</b>	<b>76.85</b>

divide the ablation experiment into the following parts based on different backbones, data augmentation strategy, fusion branches, and ablation study with SOTA. All ablation experiments are based on the pre-trained weight: ‘vit\_h’ for better performance. Besides, the FS1000 data set has very little cross-domain difficulty and is not representative, so we did not use it in ablation experiments to test the effectiveness

of our algorithms but only used it in comparative experiments in Table I.

**Backbone and Data Augmentation Ablation.** In the additional task-specific class-domain agnostic feature extraction and auto-prompts generation branch, we performed ablation experiments on the models’ performance on three data sets that are more difficult to cross-domain under 1-way 1-shot



and 5-shot settings, and the details are shown in Table II. This study proves that ResNet has a stronger recognition ability for categories, and its effect is outstanding in our novel learnable prompt.

TABLE II: Ablation Study of different backbones under 1-way 1-shot and 5-shot settings.

Backbone	ChestX		ISIC		Deepglobe	
	1-shot	5-shot	1-shot	5-shot	1-shot	5-shot
ResNet50						
w/o Data Augmentation	60.14	75.68	21.19	27.32	43.29	53.10
with Data Augmentation	70.31	88.61	54.89	73.39	46.10	61.98
HardNet85						
w/o Data Augmentation	61.30	73.70	23.40	31.72	40.98	59.73
with Data Augmentation	65.79	86.54	56.11	69.79	46.63	56.37

**Branch Ablation.** In branch ablation testing based on different backbones, we chose ResNet as the backbone of CNN-based feature extraction in CDTAP. First, MFF is multi-level feature fusion module. CDTAP is a task-adaptive information disentanglement module. Previous work of APSeg [50] and HQ-SAM [36] was set along with our method for branch ablation study, shown in Table III.

TABLE III: Ablation Study of MFF and CDTAP in 5-shot setting.

Model	Backbone	Modules		mIOU(%)				
		MFF	CDTAP	ChestX	ISIC	Deepglobe	FSS1000	Average
SAM Baseline								
SAM	ViT	✗	✗	28.80	44.55	20.19	77.90	42.86
APSeg	ViT	✗	✓	84.50	53.89	39.98	81.90	65.09
Our	ViT+ResNet	✗	✓	85.01	60.30	56.98	79.87	70.54
SAM ++								
HQ-SAM	ViT	✓	✗	30.14	47.60	26.02	80.97	46.18
APSeg	ViT	✓	✓	86.91	69.14	42.03	82.50	70.14
Our	ViT+ResNet	✓	✓	88.61	73.39	61.98	83.41	76.85

**Comparison with SOTA under the Same Setting.** To provide a fair baseline, we train PATNet with ViT-base, SAM initialization, and  $1024 \times 1024$  crops. Results in Table IV demonstrate again the superiority of our TAVP compared with PATNet under the same settings. We can see that the ViT-based PATNet improves the performance compared to CNN-based PATNet [4] on the dataset of Chest X-ray, ISIC, and Deepglobe. These results prove again that these three datasets are more challenging, and our method performs more robustly.

TABLE IV: Ablation Study of SOTA under the same setting in the 1-shot scenario.

Method	Backbone	Size	ChestX	ISIC	Deepglobe
TAVP	ViT-base	$1024 \times 1024$	70.31	<b>54.89</b>	<b>46.10</b>
PATNet	ViT-base	$1024 \times 1024$	76.43	44.25	22.37

### C. Efficiency Comparison

Considering the huge amount of parameter calculation required for the basic model, we only train some fine-tunable parameters. SAM needs to train a model with a large number

of parameters from scratch, while our framework only needs to fine-tune some layers and parameters instead of starting from scratch. In addition, linear computation is added to our framework to reduce the number of parameters, which results in our model being more parametric lightweight compared with SAM. The detailed efficiency comparison results are

TABLE V: Ablation Study of efficiency.

Backbone	Vision Encoders	#Params(M)
Hardnet	CNN	41.56
Hardnet + attention	CNN	46.14
ResNet + attention	CNN	38.54
CDTAP	CNN	<b>36.5</b>
SAM	ViT-B	93.7
SAM	ViT-L	312.3
SAM	ViT-H	641.1

TABLE VI: Efficiency Comparison between SAM based models

Method	Resolution	Learnable Parameters(M)	FPS
TAVP(our)	$1024 \times 1024$	36.5	12
SAM	$1024 \times 1024$	1191	8

shown in the Table VI. Table V shows the detailed parameter comparison. Notice that the bottom three lines are the parameters of the original SAM based on ViT. The other lines are our whole framework's parameters based on different backbones, all smaller than SAM. These results prove again that our method improves the efficiency of SAM and is more light-weighted.

## VI. CONCLUSION

It is worth noting that our work is the first one to apply a large foundation model-based method to CDFSS tasks. Previous works have focused on traditional CNN-based deep learning methods, slowing down the exploration of Artificial General Intelligence. Our method is based on SAM, a large foundational model for segmentation, concurrently rethinking its value in CDFSS. Extensive experiments have shown that although SAM can get satisfactory results for most segmentation tasks, it still performs worse in some particular scenarios, especially on the Deepglobe data set. Thus, our work has provided a novel and efficient framework for large model transfer in CDFSS tasks. The CDTAP module achieves learnable prompts for excellent performance on the three benchmarks.

In other words, SAM can be a basic knowledge tool, and using SAM to transfer its knowledge to other specific situations to complete domain-specific tasks is worthwhile. Besides, our method is an initial exploration of transferring SAM to CDFSS tasks, and many of the more critical and efficient algorithms need to be explored in the future. More methods with strong learning ability that can complete cross-domain and few-shot tasks need to be researched, helping the development of Artificial General Intelligence in the future.

## REFERENCES

- [1] L.-C. Chen, G. Papandreou, I. Kokkinos, K. Murphy, and A. L. Yuille, "Semantic image segmentation with deep convolutional nets and fully connected crfs." Piscataway, NJ, USA: Arxiv, 2014.
- [2] K. Wang, J. H. Liew, Y. Zou, D. Zhou, and J. Feng, "Panet: Few-shot image semantic segmentation with prototype alignment," in *proceedings of the IEEE/CVF international conference on computer vision*. Piscataway, NJ, USA: ICCV, 2019, pp. 9197–9206.
- [3] H. Guan and M. Liu, "Domain adaptation for medical image analysis: a survey," *IEEE Transactions on Biomedical Engineering*, vol. 69, no. 3, pp. 1173–1185, 2021.
- [4] S. Lei, X. Zhang, J. He, F. Chen, B. Du, and C.-T. Lu, "Cross-domain few-shot semantic segmentation," in *European Conference on Computer Vision*. Piscataway, NJ, USA: Springer, 2022, pp. 73–90.
- [5] G.-P. Ji, D.-P. Fan, P. Xu, M.-M. Cheng, B. Zhou, and L. Van Gool, "Sam struggles in concealed scenes—empirical study on" segment anything," 2023.
- [6] S. He, R. Bao, J. Li, P. E. Grant, and Y. Ou, "Accuracy of segment-anything model (sam) in medical image segmentation tasks," 2023.
- [7] T. Zhou, Y. Zhang, Y. Zhou, Y. Wu, and C. Gong, "Can sam segment polyps?" 2023.
- [8] B. Zhang, E. Rigall, Y. Huang, X. Zou, S. Zhang, J. Dong, and H. Yu, "A method for breast mass segmentation using image augmentation with sam and receptive field expansion," in *Proceedings of the 2023 12th International Conference on Computing and Pattern Recognition*, 2023, pp. 387–394.
- [9] H. Zhang, P. Li, X. Liu, X. Yang, and L. An, "An iterative semi-supervised approach with pixel-wise contrastive loss for road extraction in aerial images," *ACM Transactions on Multimedia Computing, Communications and Applications*, vol. 20, no. 3, pp. 1–21, 2023.
- [10] A. Kirillov, E. Mintun, N. Ravi, H. Mao, C. Rolland, L. Gustafson, T. Xiao, S. Whitehead, A. C. Berg, W.-Y. Lo *et al.*, "Segment anything," 2023.
- [11] L. Tang, H. Xiao, and B. Li, "Can sam segment anything? when sam meets camouflaged object detection," 2023.
- [12] Y. Fu, Y. Fu, and Y.-G. Jiang, "Meta-fdmixup: Cross-domain few-shot learning guided by labeled target data," in *Proceedings of the 29th ACM international conference on multimedia*, 2021, pp. 5326–5334.
- [13] Y. Liu, M. Zhu, H. Li, H. Chen, X. Wang, and C. Shen, "Matcher: Segment anything with one shot using all-purpose feature matching," 2023.
- [14] T. Leng, Y. Zhang, K. Han, and X. Xie, "Self-sampling meta sam: Enhancing few-shot medical image segmentation with meta-learning," in *Proceedings of the IEEE/CVF Winter Conference on Applications of Computer Vision*, 2024, pp. 7925–7935.
- [15] Y. Fu, Y. Xie, Y. Fu, J. Chen, and Y.-G. Jiang, "Me-d2n: Multi-expert domain decomposition network for cross-domain few-shot learning," in *Proceedings of the 30th ACM international conference on multimedia*, 2022, pp. 6609–6617.
- [16] Y.-H. Tsai, K. Sohn, S. Schuler, and M. Chandraker, "Domain adaptation for structured output via discriminative patch representations," in *Proceedings of the IEEE/CVF International Conference on Computer Vision*. Piscataway, NJ, USA: CVPR, 2019, pp. 1456–1465.
- [17] J. Hoffman, D. Wang, F. Yu, and T. Darrell, "Fcns in the wild: Pixel-level adversarial and constraint-based adaptation," 2016.
- [18] Y. Chen, W. Li, and L. Van Gool, "Road: Reality oriented adaptation for semantic segmentation of urban scenes," in *Proceedings of the IEEE conference on computer vision and pattern recognition*. Piscataway, NJ, USA: CVPR, 2018, pp. 7892–7901.
- [19] Y.-H. Tsai, W.-C. Hung, S. Schuler, K. Sohn, M.-H. Yang, and M. Chandraker, "Learning to adapt structured output space for semantic segmentation," in *Proceedings of the IEEE conference on computer vision and pattern recognition*. Piscataway, NJ, USA: CVPR, 2018, pp. 7472–7481.
- [20] Y. Zou, Z. Yu, B. Kumar, and J. Wang, "Unsupervised domain adaptation for semantic segmentation via class-balanced self-training," in *Proceedings of the European conference on computer vision (ECCV)*. Piscataway, NJ, USA: ECCV, 2018, pp. 289–305.
- [21] X. Zhu, H. Zhou, C. Yang, J. Shi, and D. Lin, "Penalizing top performers: Conservative loss for semantic segmentation adaptation," in *Proceedings of the European Conference on Computer Vision (ECCV)*. Piscataway, NJ, USA: ECCV, 2018, pp. 568–583.
- [22] Y. Zhang, P. David, H. Foroosh, and B. Gong, "A curriculum domain adaptation approach to the semantic segmentation of urban scenes," *IEEE transactions on pattern analysis and machine intelligence*, vol. 42, no. 8, pp. 1823–1841, 2019.
- [23] B. Hariharan, P. Arbeláez, L. Bourdev, S. Maji, and J. Malik, "Semantic contours from inverse detectors," in *2011 international conference on computer vision*. Piscataway, NJ, USA: IEEE, 2011, pp. 991–998.
- [24] K. Lee, H. Yang, S. Chakraborty, Z. Cai, G. Swaminathan, A. Ravichandran, and O. Dabeer, "Rethinking few-shot object detection on a multi-domain benchmark," in *European Conference on Computer Vision*. Piscataway, NJ, USA: Springer, 2022, pp. 366–382.
- [25] W.-Y. Lee, J.-Y. Wang, and Y.-C. F. Wang, "Domain-agnostic meta-learning for cross-domain few-shot classification," in *ICASSP 2022-2022 IEEE International Conference on Acoustics, Speech and Signal Processing (ICASSP)*. Piscataway, NJ, USA: IEEE, 2022, pp. 1715–1719.
- [26] L. Zhuo, Y. Fu, J. Chen, Y. Cao, and Y.-G. Jiang, "Tgdm: Target guided dynamic mixup for cross-domain few-shot learning," in *Proceedings of the 30th ACM International Conference on Multimedia*. Piscataway, NJ, USA: ACM, 2022, pp. 6368–6376.
- [27] Z. Tian, H. Zhao, M. Shu, Z. Yang, R. Li, and J. Jia, "Prior guided feature enrichment network for few-shot segmentation," *IEEE transactions on pattern analysis and machine intelligence*, vol. 44, no. 2, pp. 1050–1065, 2020.
- [28] B. Yang, C. Liu, B. Li, J. Jiao, and Q. Ye, "Prototype mixture models for few-shot semantic segmentation," in *Computer Vision—ECCV 2020: 16th European Conference, Glasgow, UK, August 23–28, 2020, Proceedings, Part VIII 16*. Piscataway, NJ, USA: Springer, 2020, pp. 763–778.
- [29] C. Zhang, G. Lin, F. Liu, J. Guo, Q. Wu, and R. Yao, "Pyramid graph networks with connection attentions for region-based one-shot semantic segmentation," in *Proceedings of the IEEE/CVF International Conference on Computer Vision*. Piscataway, NJ, USA: CVPR, 2019, pp. 9587–9595.
- [30] X. Tan, J. Xu, Y. Cao, K. Xu, L. Ma, and R. W. Lau, "Hsnet: hierarchical semantics network for scene parsing," *The Visual Computer*, vol. 39, no. 7, pp. 2543–2554, 2023.
- [31] G. Li, V. Jampani, L. Sevilla-Lara, D. Sun, J. Kim, and J. Kim, "Adaptive prototype learning and allocation for few-shot segmentation," in *Proceedings of the IEEE/CVF conference on computer vision and pattern recognition*. Piscataway, NJ, USA: ICCV, 2021, pp. 8334–8343.
- [32] W. Wang, L. Duan, Y. Wang, Q. En, J. Fan, and Z. Zhang, "Remember the difference: Cross-domain few-shot semantic segmentation via meta-memory transfer," in *Proceedings of the IEEE/CVF Conference on Computer Vision and Pattern Recognition*. Piscataway, NJ, USA: CVPR, 2022, pp. 7065–7074.
- [33] A. Tavera, F. Cermelli, C. Masone, and B. Caputo, "Pixel-by-pixel cross-domain alignment for few-shot semantic segmentation," in *Proceedings of the IEEE/CVF Winter Conference on Applications of Computer Vision*. Piscataway, NJ, USA: Springer, 2022, pp. 1626–1635.
- [34] Y. Lu, X. Wu, Z. Wu, and S. Wang, "Cross-domain few-shot segmentation with transductive fine-tuning," 2023.
- [35] Y. Wang, Z. Xu, J. Tian, J. Luo, Z. Shi, Y. Zhang, J. Fan, and Z. He, "Cross-domain few-shot learning for rare-disease skin lesion segmentation," in *ICASSP 2022-2022 IEEE International Conference on Acoustics, Speech and Signal Processing (ICASSP)*. Piscataway, NJ, USA: ICASSP, 2022, pp. 1086–1090.
- [36] L. Ke, M. Ye, M. Danelljan, Y. Liu, Y.-W. Tai, C.-K. Tang, and F. Yu, "Segment anything in high quality," *Advances in Neural Information Processing Systems*, vol. 36, pp. arXiv–2306, 2024.
- [37] C. E. Shannon, "A mathematical theory of communication," *ACM SIGMOBILE mobile computing and communications review*, vol. 5, no. 1, pp. 3–55, 2001.
- [38] F. Milletari, N. Navab, and S.-A. Ahmadi, "V-net: Fully convolutional neural networks for volumetric medical image segmentation," in *2016 fourth international conference on 3D vision (3DV)*. Piscataway, NJ, USA: international conference, 2016, pp. 565–571.
- [39] I. Demir, K. Koperski, D. Lindenbaum, G. Pang, J. Huang, S. Basu, F. Hughes, D. Tuia, and R. Raskar, "Deepglobe 2018: A challenge to parse the earth through satellite images," in *Proceedings of the IEEE Conference on Computer Vision and Pattern Recognition Workshops*. Piscataway, NJ, USA: CVPR, 2018, pp. 172–181.
- [40] N. Codella, V. Rotemberg, P. Tschandl, M. E. Celebi, S. Dusza, D. Gutman, B. Helba, A. Kallou, K. Liopyris, M. Marchetti *et al.*, "Skin lesion analysis toward melanoma detection 2018: A challenge hosted by the international skin imaging collaboration (isic)," 2019.
- [41] P. Tschandl, C. Rosendahl, and H. Kittler, "The ham10000 dataset, a large collection of multi-source dermatoscopic images of common pigmented skin lesions," *Scientific data*, vol. 5, no. 1, pp. 1–9, 2018.
- [42] S. Jaeger, A. Karargyris, S. Candemir, L. Folio, J. Siegelman, F. Callaghan, Z. Xue, K. Palaniappan, R. K. Singh, S. Antani *et al.*,

“Automatic tuberculosis screening using chest radiographs,” *IEEE transactions on medical imaging*, vol. 33, no. 2, pp. 233–245, 2013.

- [43] S. Candemir, S. Jaeger, K. Palaniappan, J. P. Musco, R. K. Singh, Z. Xue, A. Karargyris, S. Antani, G. Thoma, and C. J. McDonald, “Lung segmentation in chest radiographs using anatomical atlases with nonrigid registration,” *IEEE transactions on medical imaging*, vol. 33, no. 2, pp. 577–590, 2013.
- [44] X. Li, T. Wei, Y. P. Chen, Y.-W. Tai, and C.-K. Tang, “Fss-1000: A 1000-class dataset for few-shot segmentation,” in *Proceedings of the IEEE/CVF conference on computer vision and pattern recognition*, 2020, pp. 2869–2878.
- [45] M. Siam, B. N. Oreshkin, and M. Jagersand, “Amp: Adaptive masked proxies for few-shot segmentation,” in *Proceedings of the IEEE/CVF International Conference on Computer Vision*. Piscataway, NJ, USA: ICCV, 2019, pp. 5249–5258.
- [46] C. Zhang, G. Lin, F. Liu, R. Yao, and C. Shen, “Canet: Class-agnostic segmentation networks with iterative refinement and attentive few-shot learning,” in *Proceedings of the IEEE/CVF conference on computer vision and pattern recognition*. Piscataway, NJ, USA: CVPR, 2019, pp. 5217–5226.
- [47] M. Boudiaf, H. Kervadec, Z. I. Masud, P. Piantanida, I. Ben Ayed, and J. Dolz, “Few-shot segmentation without meta-learning: A good transductive inference is all you need?” in *Proceedings of the IEEE/CVF conference on computer vision and pattern recognition*. Piscataway, NJ, USA: CVPR, 2021, pp. 13 979–13 988.
- [48] J. Min, D. Kang, and M. Cho, “Hypercorrelation squeeze for few-shot segmentation,” in *Proceedings of the IEEE/CVF international conference on computer vision*. Piscataway, NJ, USA: ICCV, 2021, pp. 6941–6952.
- [49] Y. Huang, X. Yang, L. Liu, H. Zhou, A. Chang, X. Zhou, R. Chen, J. Yu, J. Chen, C. Chen *et al.*, “Segment anything model for medical images?” 2023.
- [50] W. He, Y. Zhang, W. Zhuo, L. Shen, J. Yang, S. Deng, and L. Sun, “Apsseg: Auto-prompt network for cross-domain few-shot semantic segmentation,” 2024.

## VII. BIOGRAPHY